Histol Histopathol (2021) 36: 425-435

http://www.hh.um.es

Histology and Histopathology
From Cell Biology to Tissue Engineering

ORIGINAL ARTICLE **Open Access**

Propofol protects PC12 cells from cobalt chloride-induced injury by mediating miR-134

Hong-Yi Zhou[1], Fan Jiang[2], Zhong Cao[1], Qi-Yun Shen[1], Yu-Jing Feng[1] and, Zhen-Huan Hou[1]

[1]Department of Anesthesiology, Tongzhou Maternal and Child Health Hospital of Beijing and

[2]Department of General Medicine, Beijing Luhe Hospital, Capital Medical University, Beijing, China

Summary. Objective. Propofol (PRO) was reported to exert a neuroprotective effect by decreasing microRNA-134 (miR-134), a brain-specific miRNA, thus, the role of PRO against cobalt chloride ($CoCl_2$)-induced injury in rat pheochromocytoma cells (PC12) via mediating miR-134 was explored.

Methods. $CoCl_2$-induced PC12 cells treated with PRO were transfected with or without miR-134 negative control (NC)/ inhibitor/mimic, and the following detections were then performed using cell counting kit-8 (CCK-8), Annexin V-fluorescein isothiocyanate/ propidium iodide (Annexin V-FITC/PI) and Hoechst 33258 staining. Autophagy was observed by transmission electron microscope (TEM). Mitochondrial membrane potential (MMP) was detected by Rhodamine-123 (Rh123) staining, and reactive oxygen species (ROS) by dichloro-dihydro-fluorescein diacetate (DCFH-DA) staining. Protein and gene expressions were measured by Western blotting and quantitative reverse transcriptase polymerase chain reaction (qRT-PCR), respectively.

Results. PRO reversed the $CoCl_2$-induced decrease in the PC12 cell viability and increased miR-134 in a dose-dependent manner. $CoCl_2$ increased LC3II/I ratio and Beclin-1 expression, but decreased p62 expression, which was abolished by PRO. In addition, an increased cell apoptosis rates triggered by $CoCl_2$ were reduced by PRO with the down-regulations of *Bax* and *Caspase-3* and the up-regulation of *Bcl-2*. Furthermore, PRO decreased methylenedioxyamphetamine (MDA), nitric oxide (NO) and ROS in $CoCl_2$-induced PC12 cells accompanying the increase in glutathione peroxidase (GSH-Px) and MMP. The effects of PRO on autophagy, apoptosis and oxidative stress in $CoCl_2$-induced PC12 cell were reversed by miR-134 mimic.

Conclusion. PRO may mitigate $CoCl_2$-induced autophagy in PC12 cells with decreased apoptosis and improved oxidative stress via mediating miR-134.

Key words: Propofol, MicroRNA-134, PC12, Cobalt chloride

Corresponding Author: Hong-Yi Zhou, Department of Anesthesiology, Tongzhou Maternal and Child Health Hospital of Beijing, 124, Yuqiao Middle Street, Tongzhou District, Beijing, China. e-mail: zhyzhy3520@163.com

DOI: 10.14670/HH-18-298

Introduction

The brain is the nerve center responsible for controlling sensation, movement and thoughts, and the maintenance of brain function depends on a normal blood supply, whereas ischemia (lack of blood supply) seriously affect brain functions (Roy and Sherrington, 1890). For example, hypoxia-ischemia brain damage (HIBD) is a complicated condition involving various factors, like free radical injury, mitochondrial damage, acute metabolic disorder of energy, and damage of inflammatory factors, finally causing cell apoptosis or necrosis (Bustelo et al., 2020; Zalewska et al., 2020). Currently, several methods, including hyperbaric oxygen treatment, mild hypothermia treatment and transplantation of neural stem cells, have been developed for HIBD (Bustelo et al., 2020; Gamdzyk et al., 2020), which, however, have not yet been applied extensively in clinical practice due to the failures in resolving their innate side-effects. Thus, the safe and effective strategies are urgently needed to improve the treatment of brain damage-related diseases.

Propofol (PRO) is a frequently applied intravenous anesthetic in the clinic with rapid induction and recovery, as well as relatively few adverse reactions (Chen et al., 2016). Recent evidence has revealed the protective effect of PRO on multiple organs during operation, involving brain, lung, spine, cardiac vessels and kidney (Kungys et al., 2009; Schrouff et al., 2011;

Adaramoye et al., 2013). According to previous studies, PRO was able to induce evident expression changes of microRNAs (miRNAs), a group of small-molecule RNAs in length of about 18 to 22 nt, thereby altering cellular biological activities (Ishikawa et al., 2012; Kim et al., 2014). For instance, PRO up-regulated miR-9 to inhibit the activation of nuclear factor-κB (NF-κB) and suppressed the expression of matrix metalloproteinase-9, thus blocking the growth and invasion of ovarian cancer cells (Huang et al., 2016). Meanwhile, PRO induced significant cell death in neurons or down-regulated several miRNAs in a dose-/time- dependent manner (Twaroski et al., 2014). MicroRNA-134 (miR-134), as a brain-specific miRNA, was critical to various biological events, including neuronal proliferation, differentiation, apoptosis and microstructural variation (Morris et al., 2018). A growing body of evidence has focused on the role of miR-134 in epilepsy. For example, Gao et al. reported that silencing miR-134 mitigated hippocampal injury in kainic acid-induced status epilepticus rats (Gao et al., 2019). A correlation of pilocarpine-induced status epilepticus in mice with the miR-134 up-regulation in hippocampus has been discovered in the work of Jimenez-Mateos et al. (2015). Also, miR-134 has been identified to sustain neuronal survival in ischemic stroke mice (Chi et al., 2014a), suggesting the potential action of miR-134 in the development of ischemia-hypoxia brain disorders. Of note, PC12 rat pheochromocytoma cell line has been widely used as a cell model in neurobiological and neurochemical studies (Gozal et al., 2017; Goloshvili et al., 2019), and PC12 cells exposed to cobalt chloride ($CoCl_2$), a well-known hypoxia mimetic agent, is an established model to investigate the mechanisms underlying neuronal cell death under the conditions of hypoxia/ischemia (Xiao et al., 2012; Hartwig et al., 2014). Considering the above, in this study, $CoCl_2$ -induced PC12 cells were used to determine the expression of miR-134 with the treatment of PRO in varying concentrations, and to further observe the changes of viability, apoptosis, autophagy and oxidative stress in PC12 cells.

Materials and methods

Cell culture

PC12 cells purchased from American Type Culture Collection (ATCC, USA) were cultured in a humidified atmosphere with with 5% CO_2 at 37°C in Dulbecco's modified eagle medium (DMEM) supplemented with 10% fetal bovine serum (FBS) and 1% streptomycin-penicillin, during which cells were passaged every one or two days. Cells in logarithmic phase were collected for subsequent experiments.

Cell viability detected by cell counting kit-8 (CCK-8)

PC12 cells (1×10^4 cells/well) were seeded in a 96-well plate, with 100 μL of medium in each well, for cultivation at 37°C with 5% CO_2. When the confluence reached 60-70%, cells were treated with $CoCl_2$ (0, 5, 10, 50, 100 μM) for 24 h, or PRO (0, 5, 10, 50, 100 μM) for 24 h followed with or without $CoCl_2$ induction (50 μM, 24 h). After incubation with 5 μL of CCK-8 solution for another 3-4 h, optical density (OD) of each well was measured at 450 nm wavelengths using a BIORAD 550 spectrophotometer (Bio-rad, California, CA, USA).

Cell grouping

Cells were divided into Normal group (cell without treatments), $CoCl_2$ group (cells treated with 50 μM of $CoCl_2$ for 24 h), PRO + $CoCl_2$ group (cells treated with 50 μM of PRO for 24 h followed by $CoCl_2$ induction), NC + $CoCl_2$ group (cells transfected with miR-134 negative control followed by $CoCl_2$ induction), inhibitor + $CoCl_2$ group (cells transfected with miR-134 inhibitor followed by $CoCl_2$ induction), PRO + NC + $CoCl_2$ group (cells transfected with miR-134 NC, followed by the treatment of PRO and $CoCl_2$) and PRO + mimic + $CoCl_2$ group (cells transfected with miR-134 mimic, followed by treatment of PRO and $CoCl_2$). PRO (R&D Systems) was dissolved in dimethlysulfoxide (DMSO) and prepared with the DMEM medium. The transfection of miR-134 mimics and inhibitors was performed according to the manufacturer's instructions of LipofectamineTM 2000 (Sigma, USA). Then, the cell viability detected by CCK-8 assay was performed as described above.

Observation of autophagy with transmission electronic microscope (TEM)

PC12 cells were cultivated at 37°C with 5% CO_2, and at confluence of about 70%-80%, cells were treated by the corresponding drugs according to the grouping requirement. The medium was discarded after 24 h, and the cells were rinsed, centrifuged and collected. In glutaric dialdehyde, cells were fixed overnight at 4°C, followed by rinses in phosphate buffer saline (PBS). Then, the cells were fixed in 1% osmic acid at 4°C, followed by dehydration and embedding in paraffin. Paraffin blocks were sliced into sections that were later stained in 3% uranyl acetate and lead citrate for observation and photographing under the transmission electronic microscope (TEM, Model 200CX, JEOL, Tokyo, Japan).

Western blotting

Total proteins were extracted from PC12 cells and then quantified by using bicinchoninic acid (BCA) protein assay kit (Pierce Biotechnology, Inc., Rockford, IL, USA). Thereafter, equal amounts of protein fractions were separated by 10% sodium dodecyl sulfate-polyacrylamide gel electrophoresis (SDS-PAGE) and then transferred onto the polyvinylidene fluoride (PVDF) membranes. Following transfer, the membranes

were blocked with 5% nonfat milk powder for 2 h at room temperature and incubated with anti-LC3I/II antibody at 2 μg/mL (ab128025, Abcam, UK), anti-Beclin-1 antibody at 1/1000 dilution (ab210498, Abcam, UK), anti-p62 antibody at 1/1000 dilution (ab109012, Abcam, UK), and anti-GAPDH antibody-loading control at 1/2500 dilution (ab9485, Abcam, UK) at 4°C overnight, which was terminated by rinsing with PBS three times (10 min/time). Thereafter, the resultant immunoblots were further incubated with the goat anti-rabbit IgG H&L (HRP) at 1 μg/mL (ab205718, Abcam, UK) for 2 h and the incubation was also ended by rinsing in PBS three times (15 min/time). The proteins were visualized by an enhanced chemiluminiscence (ECL) detection system (Amersham Biosciences Corp., Piscataway, NJ, USA). The intensity of each band was quantified with the Image reader software (Science Lab software, Fuji Photo Film, Tokyo, Japan).

Annexin-V fluorescein isothiocyanate/propidium iodide (Annexin V-FITC/PI) staining

PC12 cells were rinsed in PBS once, and detached in EDTA-free trypsin, which was terminated by adding the serum-contained medium. The cells (1×10^6/mL) were centrifuged at 12000 rpm for 5 min followed by rinsing with PBS. Subsequently, cells were washed by binding buffer (500 μL) and then mixed with 5 μL of Annexin-V-FITC and 5 μL of PI, followed by incubation in the dark at room temperature for 15 min. Cells were then subjected to the measurement by using a flow cytometer (Amnis Corp., Seattle, USA). The apoptosis rate was calculated as early apoptosis (lower, right) + late apoptosis (upper, right) (Cai et al., 2014).

Hoechst 33258 staining

PC12 cells were rinsed in PBS three times (3 min/time), and fixed in 4% paraformaldehyde for 10 min. Then, the cells were washed in PBS three times and incubated with 500 μL of Hoechst 33258 in the dark at 4°C for 10 min. Following three washes with PBS, cell morphology was observed and photographed under an Olympus IX-70 fluorescent microscope (Center Valley, PA, USA).

Quantitative reverse transcriptase polymerase chain reaction (qRT-PCR)

The total RNA was extracted from PC12 cells using the TRIzol reagent (Invitrogen, Carlsbad, CA, USA). The first-strand cDNAs were synthesized by using the PrimeScript® II 1st Strand cDNA Synthesis Kit (Takara Bio Inc. Otsu, Japan). Then, qRT-PCR was performed using a QuantStudio™ 6 Real-Time PCR detection system (Thermo Fisher Scientific, Foster, CA, USA) with the reaction condition of 10 min at 95°C followed by 40 cycles of 15 s at 95°C (denaturation step) and 30 s at 60°C (annealing/extension step). The relative expressions of miR-134, Bax, Caspase-3 and Bcl-2 in PC12 cells were calculated using the $2^{-\Delta\Delta CT}$ method (Arocho et al., 2006).

Rhodamine 123 (Rh123) staining

Cells were fixed in 4% paraformaldehyde for 15 min, which was ended by three washes with PBS. In each well, the cells were then incubated with Rh123 in a final concentration (10 μmol/L) at 37°C without light for 30 min, and incubation was terminated by washes in PBS. Sections were mounted in 50% glycerol, and observed under a laser-scanning confocal microscope (Nikon Eclipse tE2000-U, Nikon Inc., Melville, NY). The percentage of positive cells was calculated by using Image J software (National Institute of Mental Health, Bethesda, Maryland, USA).

Detection of oxidative stress indicators

Commercial kits (Nanjing Jiancheng Bioengineering Institute, China) were used to detect the methylenedioxyamphetamine (MDA), nitric oxide (NO) and glutathione peroxidase (GSH-Px) levels. Reactive oxygen species (ROS) levels were determined using dichloro-dihydro-fluorescein diacetate (DCFH-DA) staining. In brief, cells were placed into the 24-well plates for 24 h of culture, and the supernatant was discarded. Following three washes in PBS, cells were fixed in 4% paraformaldehyde for 15 min. Again, cells were washed with PBS three times, and then incubated with DCFH-DA in a final concentration (10 μmol/L) at 37°C for 30 min avoiding exposure to light. Cells were rinsed in PBS, and were mounted in 50% glycerol. Then, the cells were observed under the laser-scanning confocal microscope (Nikon Eclipse tE2000-U, Nikon Inc., Melville, NY), and the percentage of positive cells was calculated by Image J software (National Institute of Mental Health, Bethesda, Maryland, USA).

Statistical analysis

SPSS 21.0 software (SPSS, Inc, Chicago, IL, USA) was used to perform the statistical analysis for data of this study. Measurement data expressed in mean ± standard deviation (SD) were compared by analysis of variance (one-way ANOVA) followed by Tukey's honestly significant difference (HSD) test. $P<0.05$ suggested that the difference had statistical significance.

Results

Effect of $CoCl_2$ and PRO in different concentrations on PC12 cell viability

CCK-8 assay revealed that $CoCl_2$ caused an significant decrease in PC12 cell viability in a concentration-dependent manner, and approximately 45% reduction was observed after 24 h with the

treatment of 50 μM $CoCl_2$, which, therefore, was selected as the final concentration for the following experiments (Fig. 1A). However, PRO in different concentrations showed no evident effects on the viability of PC12 cells (Fig. 1B), which reversed the decreased PC12 cell viability caused by 50 μM of $CoCl_2$ treatment for 24 h in a dose-dependent manner (Fig. 1C).

Effect of PRO on miR-134 expression in $CoCl_2$-induced PC12 cells

$CoCl_2$ up-regulated miR-134 expression in PC12 cells in a dose-dependent manner (Fig. 2A), but after the pre-treatment of PRO (5, 10, 50, 100 μM), the up-regulation of miR-134 induced by 50 μM of $CoCl_2$ was dose-dependently reversed in PC12 cells (all $P<0.05$, Fig. 2B).

Effect of PRO on the viability of $CoCl_2$-treated PC12 cells by mediating miR-134

MiR-134 expression in PC12 cells was determined by using qRT-PCR (Fig. 3A). As compared with the $CoCl_2$ group, miR-134 was down-regulated in the PC12 cells from Normal group, PRO + $CoCl_2$ group, inhibitor + $CoCl_2$ group and PRO + NC + $CoCl_2$ group (all $P<0.05$), but was not significantly different from NC + $CoCl_2$ group and PRO + mimic + $CoCl_2$ group, as well as PRO + $CoCl_2$ group and PRO + NC + $CoCl_2$ group (all $P>0.05$). Besides, Normal group and inhibitor + $CoCl_2$ group also showed no significant difference in

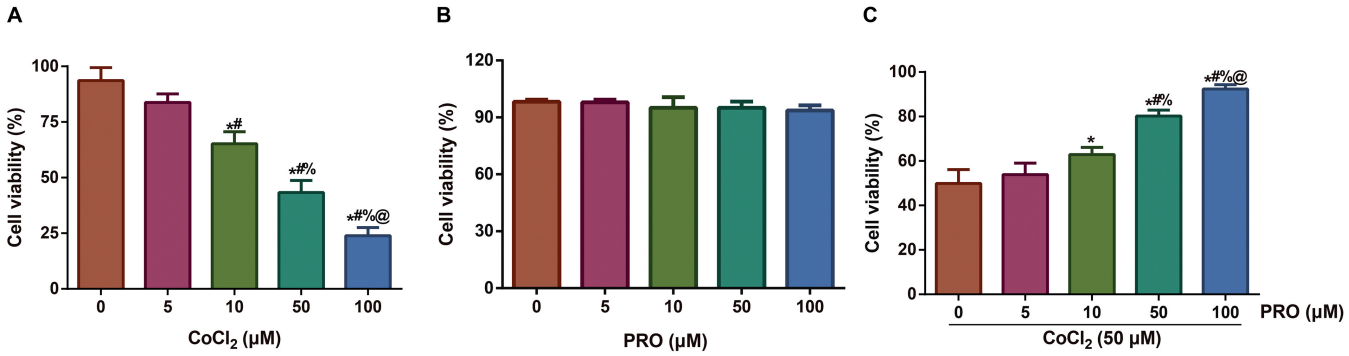

Fig. 1. The effects of $CoCl_2$ and PRO in different concentrations on PC12 cell viability evaluated by CCK-8 assay. **A.** $CoCl_2$ (0, 5, 10, 50, 100 μM) decreases the viability of PC12 cells in a dose-dependent manner. **B.** Treatment of PRO in varying concentrations (0, 5, 10, 50, 100 μM) caused no effect on the viability of PC12 cells;.**C.** PRO (0, 5, 10, 50, 100 μM) reverses the decreases caused by treatment of $CoCl_2$ (50 μM, 24 h) in PC12 cell viability in a dose-dependent manner. This experiment was conducted in triplicate. *: $P<0.05$ vs. 0 μM, #: $P<0.05$ vs. 5 μM, %: $P<0.05$ vs. 10 μM, @: $P<0.05$ vs. 50 μM.

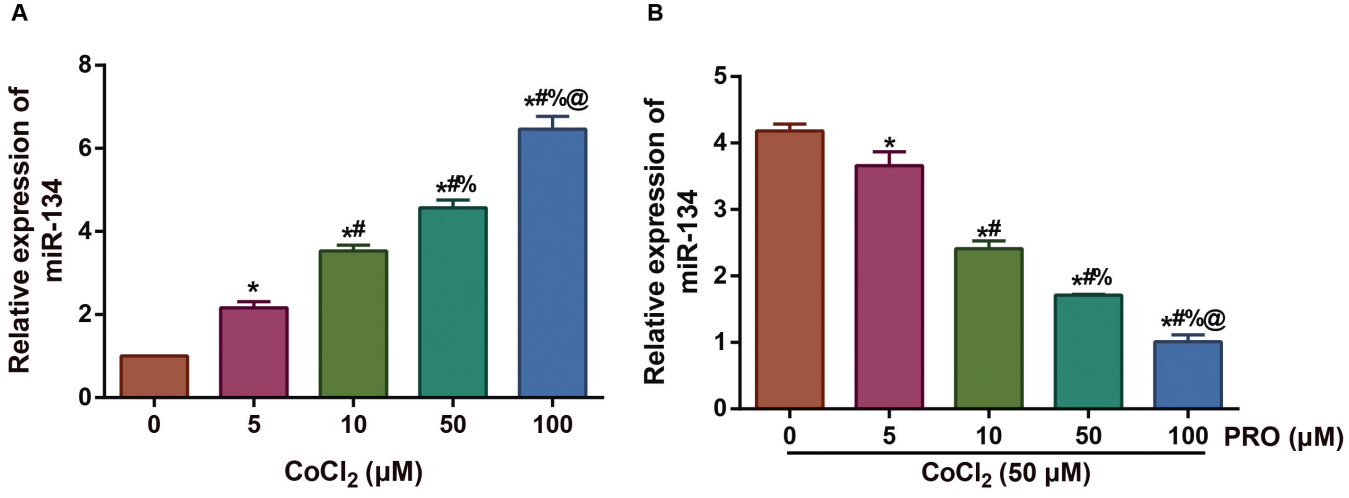

Fig. 2. Effect of different concentrations of PRO on miR-134 expression in $CoCl_2$-treated PC12 cells. This experiment was conducted in triplicate. *: $P<0.05$ vs. 0 μM, #: $P<0.05$ vs. 5 μM, %: $P<0.05$ vs. 10 μM, @: $P<0.05$ vs. 50 μM.

miR-134 expression. CCK-8 assay (Fig. 3B) revealed that PC12 cell viability was the highest in the Normal group, which was decreased by the treatment with $CoCl_2$, and both PRO and miR-134 inhibitor enhanced the PC12 cell viability induced by $CoCl_2$ (all $P<0.05$). No significant differences were observed concerning the PC12 cell viability among PRO + $CoCl_2$ group, PRO + NC + $CoCl_2$ group and inhibitor + $CoCl_2$ group, or among $CoCl_2$ group, NC + $CoCl_2$ group and PRO + mimic + $CoCl_2$ group (all $P<0.05$).

Effect of PRO on the autophagy of $CoCl_2$-treated PC12 cells by mediating miR-134

According to the TEM observation in Figure 4A, as compared with the Normal group, evident increases in the autophagy of PC12 cells were found in the other groups, but PRO treatment resulted in decreased autophagy in PC12 cells caused by $CoCl_2$ when compared with those treated with $CoCl_2$ alone, which was reversed by miR-134 mimic. The expressions of autophagy-related makers detected by western blotting (Fig. 4B-E) revealed that $CoCl_2$-induced PC12 cells exhibited an obvious elevation of LC3II/LC3I ratio and Beclin-1 expression, as well as the down-regulation of p62 expression when compared with the Normal group (all $P<0.05$). However, PRO treatment and miR-134 inhibitor transfection decreased LC3II/LC3I and Beclin-1 with the increased p62 in $CoCl_2$-induced PC12 cells (all $P<0.05$). The levels of autophagy-associated proteins showed no statistical significance among $CoCl_2$ group and PRO + mimic + $CoCl_2$ group (all $P>0.05$).

Effect of PRO on the apoptosis of $CoCl_2$-treated PC12 cells by mediating miR-134

Hoechst 33258 staining revealed that the treatment of PRO or the transfection of miR-134 inhibitor reversed the karyopyknosis and nuclear fragmentation caused by $CoCl_2$ (Fig. 5A). Annexin V-FITC/PI staining was applied to validate the apoptosis of PC12 cells (Fig. 5B-C), and as a result, the PC12 cells after $CoCl_2$ induction had the increased apoptosis rate comapred with the Normal group, and the apoptosis rate in the $CoCl_2$ group was far higher than that in the PRO + $CoCl_2$ group or the inhibitor + $CoCl_2$ group (both $P<0.05$). Furthermore, the decresed apoptosis rate treated by PRO in $CoCl_2$-treated PC12 cells was revesed by miR-134 mimic ($P<0.05$). Similarly, qRT-PCR (Fig. 6) also demonstrated that $CoCl_2$ induction increased the expressions of Bax and Caspase-3 and decresed Bcl-2 expression, but PRO or miR-134 inhibitor decreased the expressions of Bax and Caspase-3 induced by $CoCl_2$ with enhanced Bcl-2 expression. As compared with the PRO + $CoCl_2$ group, PC12 cells in the PRO + mimic + $CoCl_2$ group presented with an evident increase in Bax and Caspase-3 expression, and a decrease in Bcl-2 expression (all $P<0.05$).

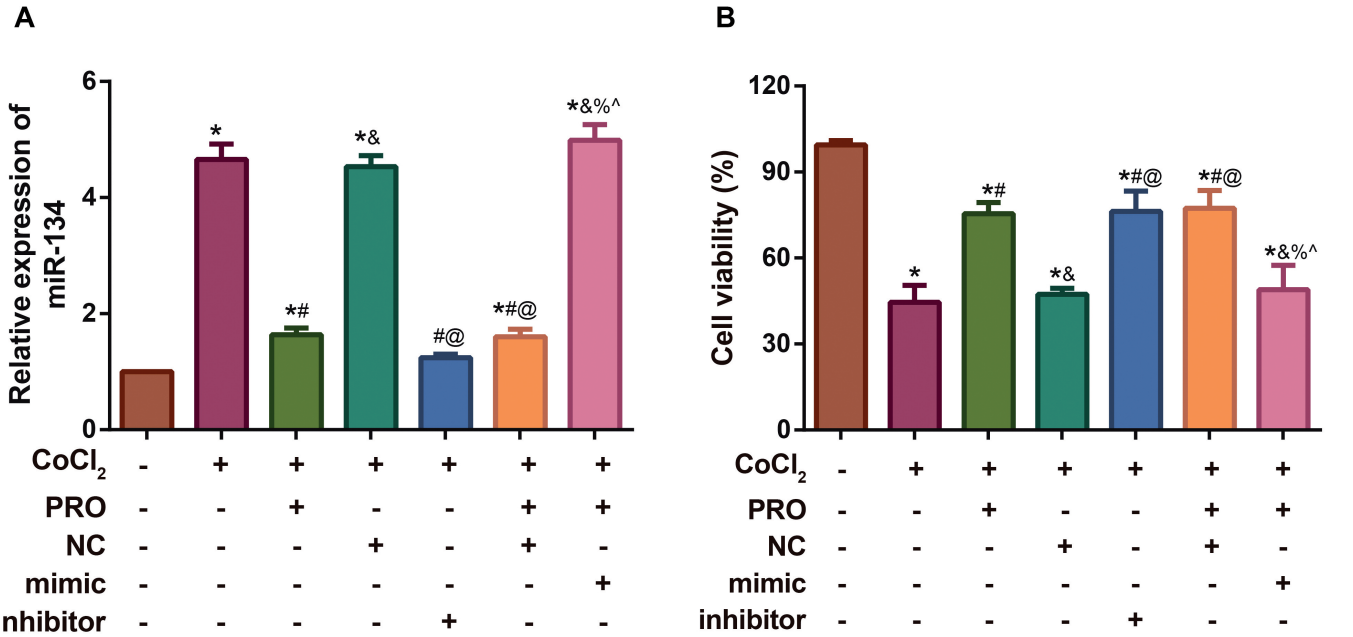

Fig. 3. Effect of PRO on the viability of $CoCl_2$-treated PC12 cells by mediating miR-134. **A.** The comparison of miR-134 expression in PC12 cells among the groups. **B.** Effect of PRO on the viability of $CoCl_2$-treated PC12 cells by mediating miR-134. This experiment was repeated three times. *: $P<0.05$ vs. normal group; #: $P<0.05$ vs. $CoCl_2$ group; &: $P<0.05$ vs. PRO + $CoCl_2$ group; @: $P<0.05$ vs. NC + $CoCl_2$ group; %: $P<0.05$ vs. inhibitor + $CoCl_2$ group; ^: $P<0.05$ vs. PRO + NC + $CoCl_2$ group; NC, miRNA negative control.

Effect of PRO on the oxidative stress of $CoCl_2$-treated PC12 cells by mediating miR-134

As shown in Figure 7, in comparison with the Normal group, $CoCl_2$ induced the increases in NO and MDA levels in PC12 cells with the reduced activity of GSH-px, which could be partly reversed by PRO and miR-134 inhibitor (all $P<0.05$). Besides, PC12 cells in the PRO + mimic + $CoCl_2$ group also had increased NO and MDA levels and decreased GSH-px activity as compared with the PRO + $CoCl_2$ group (all $P<0.05$). Furthermore, decreased fluorescence intensity of Rh123 was found in $CoCl_2$-treated PC12 cells (all $P<0.05$, Fig. 8A-B), and it was increased after the treatment with PRO, which, however, were partially reversed by transfection of miR-134 mimic (all $P<0.05$). As compared to Normal group, the other groups had the increased ROS level (all $P<0.05$, Fig. 8C-D). ROS levels in PC12 cells in PRO + $CoCl_2$ group and inhibitor + $CoCl_2$ group were decreased evidently as compared with those treated with $CoCl_2$ alone (both $P<0.05$), which was much higher in PRO + mimic + $CoCl_2$ group compared to PRO + $CoCl_2$ group ($P<0.05$).

Discussion

In this study, the PC12 cells exhibited declined cell viability dose-dependently after induction with different concentrations of $CoCl_2$. Previous studies have shown that a cell death rate of 40-60% is a promising option to study the neuroprotective effect of drugs, whereas an excessively high death rate may limit function, thereby making it difficult to clarify the pathogenesis (Lahiani et al., 2015, 2016). Thus, 50 μM of $CoCl_2$ induction was selected as the final concentration for our following experiments. As we know, miR-134 is specifically expressed in the brain tissues (Morris et al., 2018). In our study, the increased $CoCl_2$ dose-dependently induced

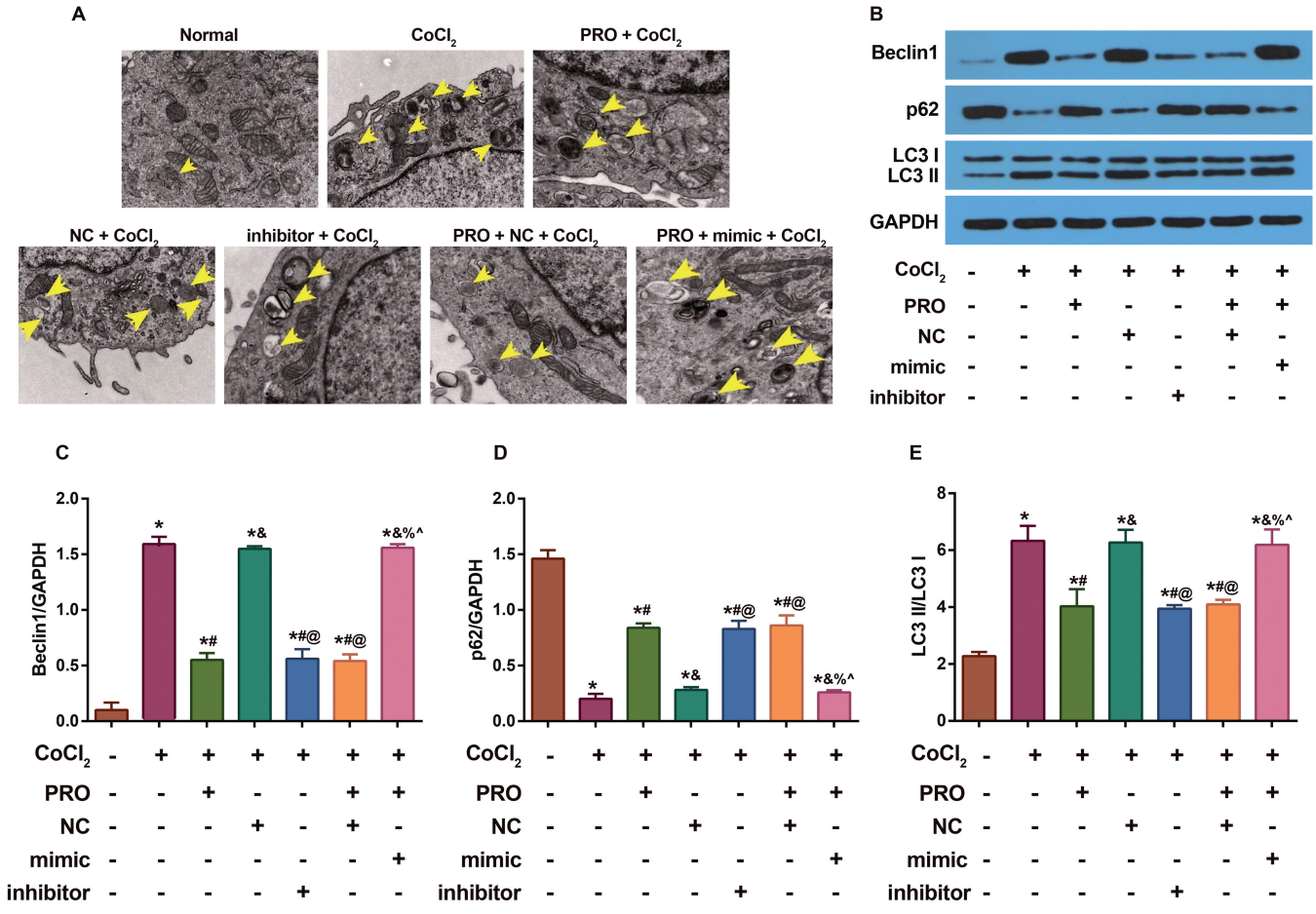

Fig. 4. Effect of PRO on the autophagy of $CoCl_2$-treated PC12 cells by mediating miR-134. **A.** Autophagic structure of PC12 cells in all groups determined by transmission electronic microscope (TEM), and arrows show various forms of autophagic vacuoles including autophagosomes and autolysosomes; **B-E.** Expressions of autophagy-associated proteins (LC3II/LC3I ratio, Beclin-1 and p62) in PC12 cells of all groups determined by Western blotting; Experiment was carried out in triplicate. *: $P<0.05$ vs. normal group; #: $P<0.05$ vs. $CoCl_2$ group; &: $P<0.05$ vs. PRO + $CoCl_2$ group; @: $P<0.05$ vs. NC + $CoCl_2$ group; %: $P<0.05$ vs. inhibitor + $CoCl_2$ group; ^: $P<0.05$ vs. PRO + NC + $CoCl_2$ group; NC, miRNA negative control.

miR-134 expression in PC12 cells, supporting the protection of miR-134 inhibition against neuron cell death under the conditions of hypoxia/ischemia as reported by other studies (Chi et al., 2014b; Meng et al., 2016; Rodriguez et al., 2017). Recently, evidence demonstrated the reduced miR-134 expression by PRO in primary hippocampal neurons under oxygen-glucose deprivation (OGD) condition (Wang et al., 2015). Similarly, we also found the up-regulation of miR-134 induced by 50 μM of $CoCl_2$ was reversed in PC12 cells after the pre-treatment of PRO, suggesting the protection role of PRO in $CoCl_2$ -induced PC12 cells via mediating

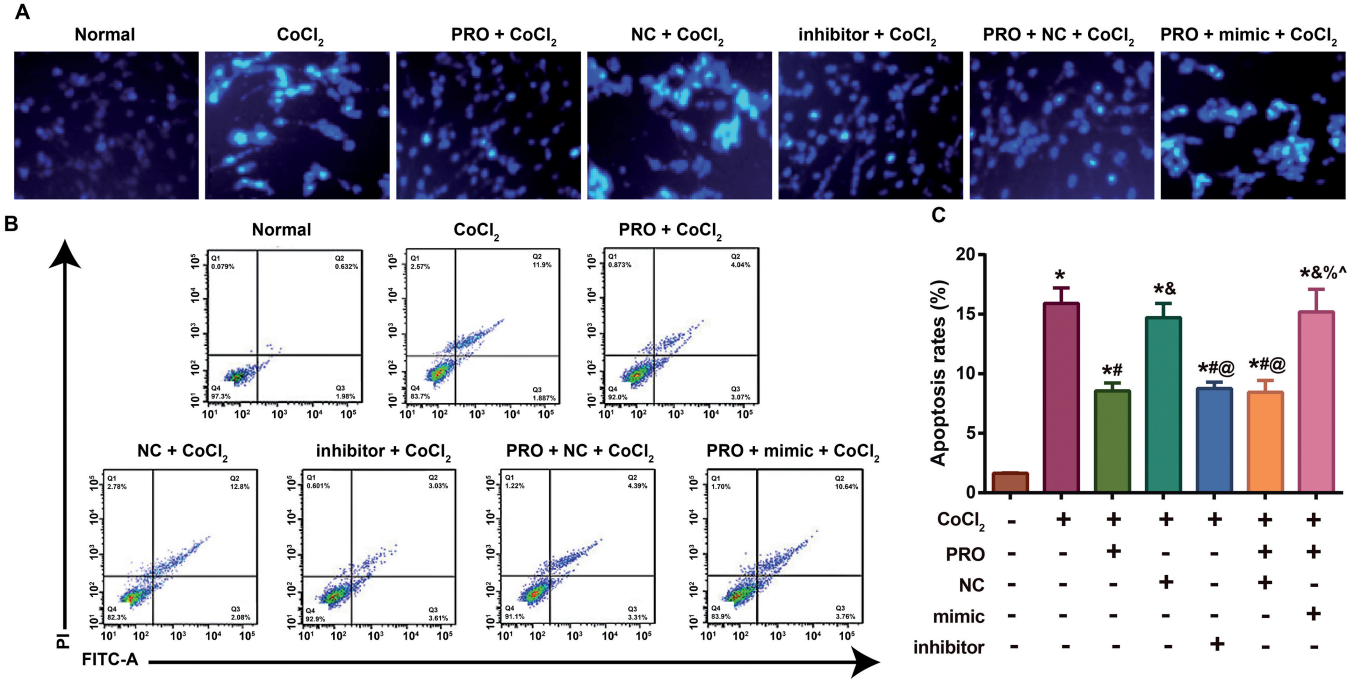

Fig. 5. Effect of PRO on the apoptosis of $CoCl_2$-treated PC12 cells by mediating miR-134. **A.** Apoptosis of PC12 cells in different groups detected by Hoechst 33258 staining; B-C: PC12 cells apoptosis validated by Annexin V-FITC/PI staining (**B**), and the comparison of PC12 cells apoptosis rate (%) among the groups (**C**). This experiment was carried out in triplicate. *: P<0.05 vs. normal group; #: P<0.05 vs. $CoCl_2$ group; &: P 0.05 vs. PRO + $CoCl_2$ group; @: P<0.05 vs. NC + $CoCl_2$ group; %: P<0.05 vs. inhibitor + $CoCl_2$ group; ^: P<0.05 vs. PRO + NC + $CoCl_2$ group; NC, miRNA negative control.

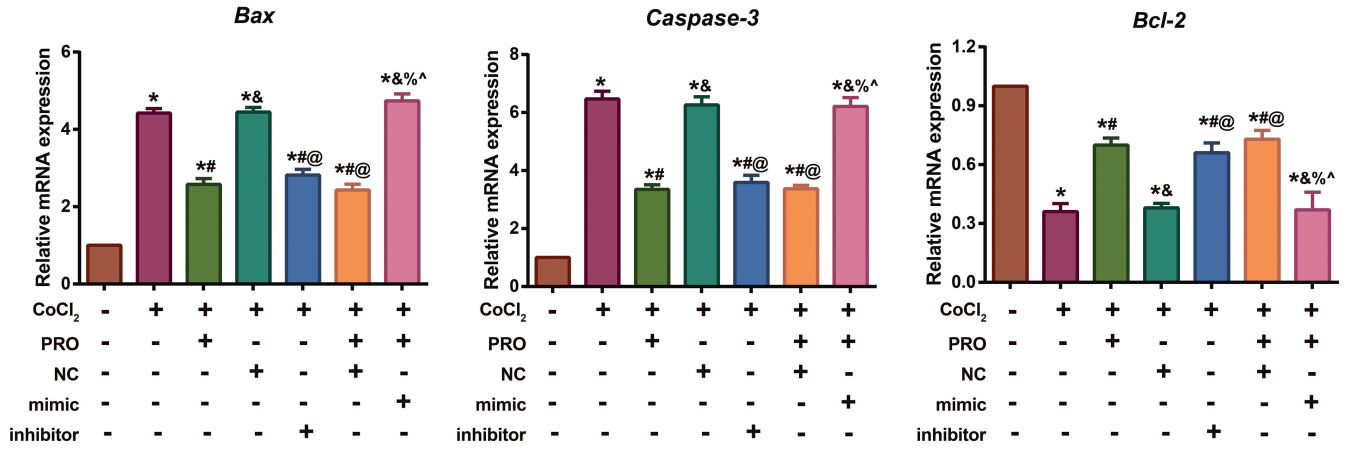

Fig. 6. Expressions of Bax, Caspase-3 and Bcl-2 in PC12 cells of different groups detected by qRT-PCR. This experiment was conducted in triplicate. *: P<0.05 vs. normal group; #: P<0.05 vs. $CoCl_2$ group; &: P<0.05 vs. PRO + $CoCl_2$ group; @: P<0.05 vs. NC + $CoCl_2$ group; %: P<0.05 vs. inhibitor + $CoCl_2$ group; ^: P<0.05 vs. PRO + NC + $CoCl_2$ group; NC, miRNA negative control.

miR-134 expression. Interestingly, the microarray analysis carried out by Kim JH et al. found the expression of miR-134 in the adipose-derived stromal cells could be elevated by 4 to 5 times after induction of PRO (Kim et al., 2014). The reason for the contrary condition may be the difference in cell types.

Autophagy, as a dynamic physiological process, plays a key role in the maintenance of cellular homeostasis (Uchiyama, 2001), which can be induced by various extracellular stimuli, including nutrition deficiency, hypoxia, high temperature and microgravity environment, as well as intracellular stimuli, like damage to the organs (Yamanaka-Tatematsu et al., 2013). Notably, $CoCl_2$ has been found to increase cell autophagy (Chimeh et al., 2018), and Beclin-1 was up-regulated in cerebral ischemia/reperfusion injury simulated by $CoCl_2$-induced HT22 cells (Yang et al., 2015). During the process of autophagy, soluble LC3-I may bind covalently to phosphatidyl ethanolamine to form LC3-II, which may further bind to the membrane of autophagosome, with the continuous decrease in LC3-I and the increase of LC3-II; therefore, the intracellular LC3-II/LC3-I ratio has been used to evaluate the development and degree of autophagy (Nakashima et al., 2006). P62/SQSTM1, the substrate of autophagy, is believed to be associated with the activation of autophagy (Bjorkoy et al., 2005). In this work, after $CoCl_2$ induction, PC12 cells presented an increase in LC3II/LC3I ratio, the up-regulation of Beclin-1 and the down-regulation of p62, indicating the increase in autophagy; however, the above changes were clearly reversed after PRO treatment. Likewise, Cui DR et al. reported that PRO may significantly inhibit the up-regulations of LC3-II and Beclin-1 in the hippocampus of I/R rat (Cui et al., 2013). The findings of Sun B et al. also showed that PRO was able to suppress OGD/R-induced autophagy and neuronal damage, manifesting with decreased LC3-II/LC3-I ratio and Beclin-1 expression, increased p62 expression, as well as declined LC3-I point-like structure (Sun et al., 2018). In this study, PRO was noted to down-regulate the increased expression of miR-134 induced by $CoCl_2$ in PC12 cells, similar to the previous findings (Kim et al., 2014; Wang et al., 2015). Furthermore, the decreased expression of miR-134 was reported to be able to down-regulate the expressions of autophagy-associated proteins in hippocampus (Sun et al., 2017). Hence, we inferred that PRO may mitigate $CoCl_2$-induced increase in the autophagy of PC12 cells via mediating miR-134.

Accumulating evidence has confirmed the PC12 cell apoptosis induced by $CoCl_2$ (Kasai et al., 2017; Wang et al., 2018). Mechanically, apoptosis usually results in damage to the MMP, and decreased MMP has been recognized widely as an early hallmark for cell apoptosis (Richter, 1993). Bcl-2, the anti-apoptotic gene located in mitochondria, is responsible for the maintenance of the integrity of the mitochondrial membrane, while Bax, the pro-apoptotic protein, can augment the permeability of mitochondrial membrane and decrease MMP to initiate apoptosis (Hajiahmadi et al., 2015). Activated caspase-3, a hallmark protein of cell apoptosis, can also trigger the initiation of mitochondrial apoptosis (Medina et al., 1997). Consequently, PRO decreased the expressions of Bax and Caspase-3 in PC12 cells treated with $CoCl_2$ in our work, accompanied with the increased Bcl-2 and MMP. As indicated by Engelhard et al., Bax expression was lower in PRO anaesthetized rats after cerebral ischaemia than in control animals (Engelhard et al., 2004). Chen XH et al. pre-treated the PC12 cells with PRO, while the apoptotic rate of PC12 cells following subsequent treatment of H2O2 was somehow decreased, with the down-regulation of caspase-3 (Chen et al., 2016). Taken together, the ability of PRO to limit $CoCl_2$-induced apoptosis in PC12 cells might be realized by

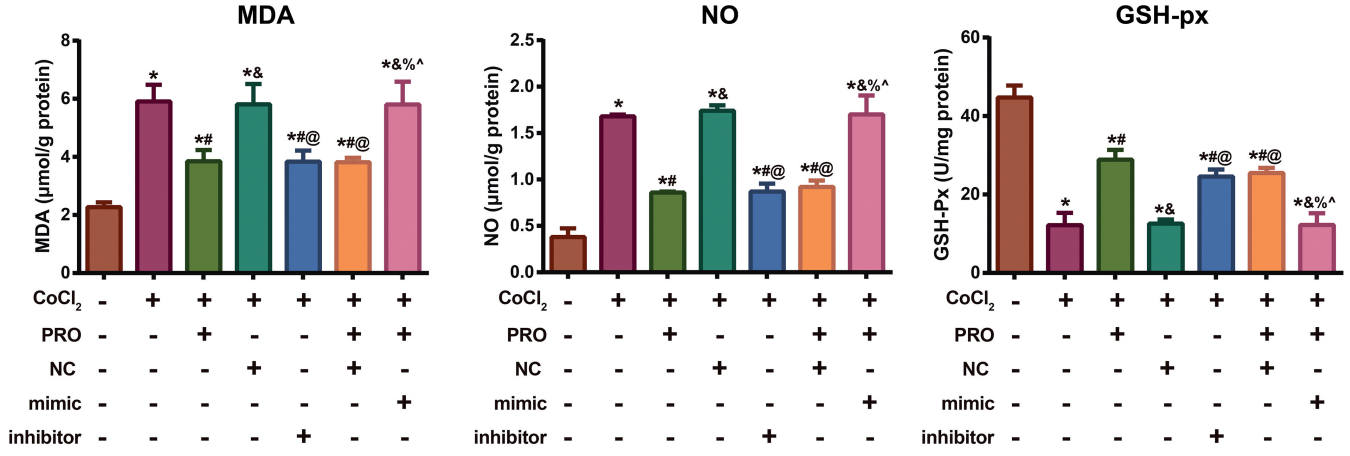

Fig. 7. Effect of PRO on the levels of methylenedioxyamphetamine (MDA), nitric oxide (NO), glutathione peroxidase (GSH-Px) in $CoCl_2$-treated PC12 cells by mediating miR-134. This experiment was repeated three times. *: P<0.05 vs. normal group; #: P<0.05 vs. $CoCl_2$ group; &: P<0.05 vs. PRO + $CoCl_2$ group; @: P<0.05 vs. NC + $CoCl_2$ group; %: P<0.05 vs. inhibitor + $CoCl_2$ group; ^: P<0.05 vs. PRO + NC + $CoCl_2$ group; NC, miRNA negative control.

mitochondrial apoptosis. In addition, as compared with the PRO + $CoCl_2$ group, PC12 cell apoptosis was enhanced in the PRO + mimic + $CoCl_2$ group, suggesting that miR-134 overexpression may reverse the effect of PRO on the $CoCl_2$-induced PC12 cell apoptosis. Consistently, the published literatures also illustrated that overexpression of miR-134 exacerbated cell apoptosis both in vitro and in vivo, and the down-regulation of miR-134 exerted neuroprotection against ischemic injury (Chi et al., 2014b). Besides, inhibition of miR-134, as reported by Huang W et al., was able to up-regulate the expression of Bcl-2 in neurons after cerebral ischemic injury (Huang et al., 2015).

Besides, the excessive generation of ROS from the mitochondrial respiratory chain could be frequently seen under the hypoxic environment (Sada et al., 2016). Thus, the levels of ROS in PC12 cells were detected, and $CoCl_2$ induction led to the increased ROS levels, with decreased green fluorescence intensity of Rh123. Meanwhile, the increased levels of NO and MDA were also confirmed with the evidently decreased GSH-px activity in this study. MDA, the final product in the process where oxygen radials destroy the membrane structure, can reflect the damage of radicals to the cells (Wohaieb and Godin, 1987). GSH-px is the general name of an enzyme family with peroxidaseactivity whose main biological role is to protect the organism from oxidative damage. (Guidi et al., 1986). As for PRO, it has a structure similar to that of butylated hydroxytoluene, which can antagonize the free radicals and suppress the lipid peroxidation (Cui et al., 2012; Chen et al., 2016). In our study, the increased oxidative stress of PC12 cells induced by $CoCl_2$ was attenuated by PRO, which was reversed by miR-134 mimic. Similarly, evidence has supported that PRO was capable of mitigating hypoxia-caused oxidative stress in brain tissues, and inhibiting miR-134 can also improve the oxidative stress in hippocampus and the mitochondrial functions (Sun et al., 2017). Besides, Wang and his group found suppression of miR-134 decreased the ROS

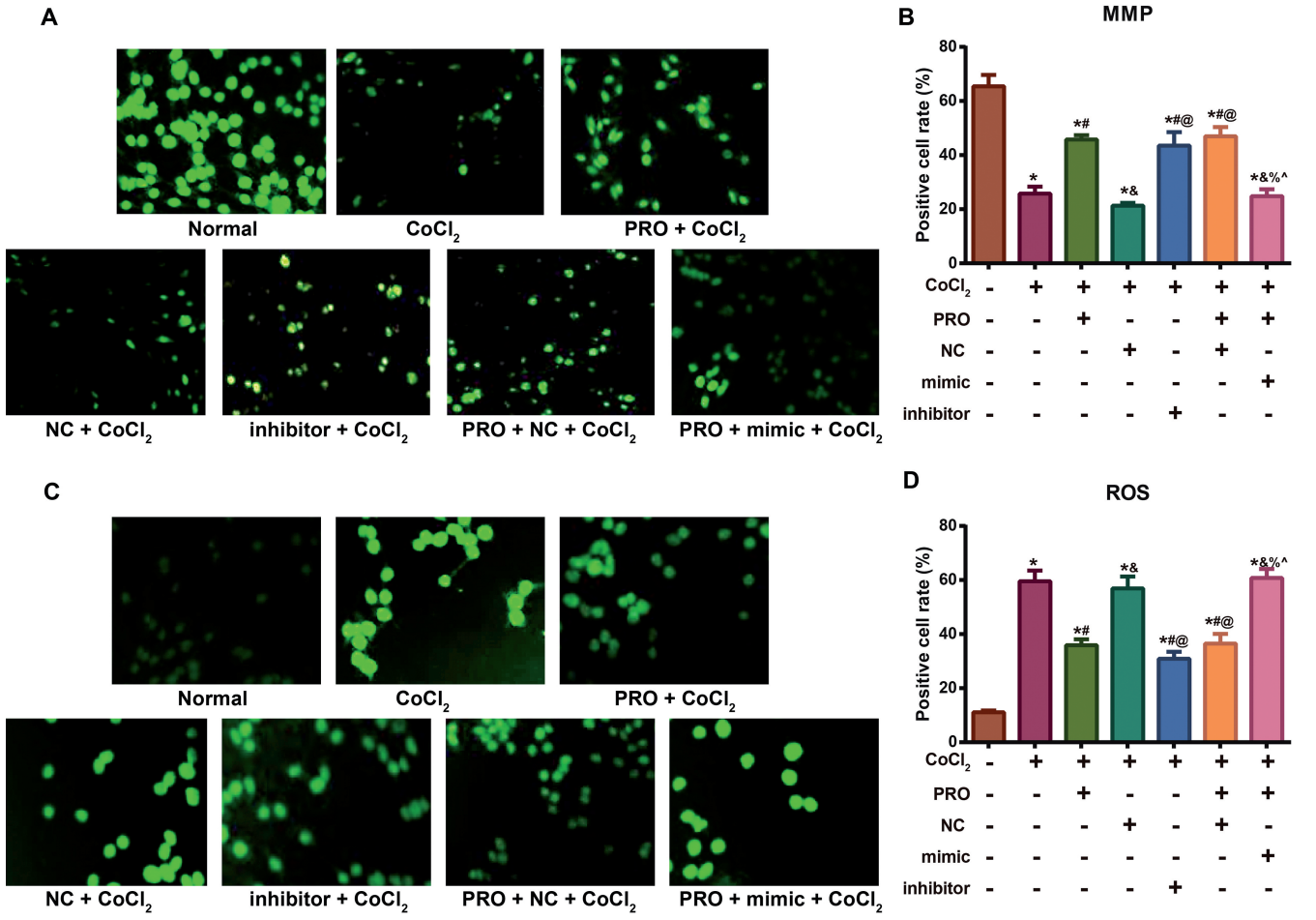

Fig. 8. Effect of PRO on the mitochondrial membrane potential (MMP) and reactive oxygen species (ROS) in $CoCl_2$-treated PC12 cells by mediating miR-134. **A-B.** Rh123 staining were performed to determine the MMP. **C-D.** ROS was examined using DCF-DA staining. This experiment was carried out in triplicate. *: P<0.05 vs. normal group; #: P<0.05 vs. $CoCl_2$ group; &: P<0.05 vs. PRO + $CoCl_2$ group; @: P<0.05 vs. NC + $CoCl_2$ group; %: P<0.05 vs. inhibitor + $CoCl_2$ group; ^: P<0.05 vs. PRO + NC + $CoCl_2$ group; NC, miRNA negative control.

levels by activating the mitochondrial respiratory chain and increasing the increased activity of antioxidant enzymes related to CREB binding, thereby decreasing apoptosis (Wang et al., 2020). All mentioned above indicating that miR-134 inhibition may have antioxidant activity in reducing or possibly preventing neuronal injury. Thus, PRO may improve the oxidative stress via mediating miR-134 in $CoCl_2$-induced PC12 cells.

In conclusion, PRO was able to decrease the expression of miR-134 in $CoCl_2$-treated PC12 cells in a dose-dependent manner. Furthermore, PRO could mitigate the $CoCl_2$-induced autophagy, apoptosis and oxidative stress in PC12 cells via inhibiting miR-134, thereby exerting a therapeutic role in the treatment of brain damage-related diseases. However, there existed a limitation that the interactions of autophagy, apoptosis and oxidative stress were complicated, which should be further explored in the future study due to time and funding constraints.

Acknowledgements. We appreciate all the reviewers for their helpful suggestions in this work.

Competing interests. The authors declare that they have no conflict of interest.

References

Adaramoye O.A., Akinwonmi O. and Akanni O. (2013). Effects of propofol, a sedative-hypnotic drug, on the lipid profile, antioxidant indices, and cardiovascular marker enzymes in wistar rats. ISRN Pharmacol. 2013, 230261.

Arocho A., Chen B., Ladanyi M. and Pan Q. (2006). Validation of the 2-deltadeltact calculation as an alternate method of data analysis for quantitative PCR of BCR-ABL P210 transcripts Diagn. Mol. Pathol. Part B. 15, 56-61.

Bjorkoy G., Lamark T., Brech A., Outzen H., Perander M., Overvatn A., Stenmark H. and Johansen T. (2005). P62/SQSTM1 forms protein aggregates degraded by autophagy and has a protective effect on huntingtin-induced cell death. J. Cell Biol. 171, 603-614.

Bustelo M., Barkhuizen M., van den Hove D.L.A., Steinbusch H.W.M., Bruno M.A., Loidl C.F. and Gavilanes A.W.D. (2020). Clinical implications of epigenetic dysregulation in perinatal hypoxic-ischemic brain damage. Front. Neurol. 11, 483.

Cai N., Zhao X., Jing Y., Sun K., Jiao S., Chen X., Yang H., Zhou Y. and Wei L. (2014). Autophagy protects against palmitate-induced apoptosis in hepatocytes. Cell Biosci. 4, 28.

Chen X.H., Zhou X., Yang X.Y., Zhou Z.B., Lu D.H., Tang Y., Ling Z.M., Zhou L.H. and Feng X. (2016). Propofol protects against H_2O_2-induced oxidative injury in differentiated PC12 cells via inhibition of Ca(2+)-dependent NADPH oxidase. Cell. Mol. Neurobiol. 36, 541-551.

Chi W., Meng F., Li Y., Li P., Wang G., Cheng H., Han S. and Li J. (2014a). Impact of microRNA-134 on neural cell survival against ischemic injury in primary cultured neuronal cells and mouse brain with ischemic stroke by targeting HSPA12B. Brain Res. 1592, 22-33.

Chi W., Meng F., Li Y., Wang Q., Wang G., Han S., Wang P. and Li J. (2014b). Downregulation of miRNA-134 protects neural cells against ischemic injury in N2A cells and mouse brain with ischemic stroke by targeting HSPA12B. Neuroscience 277, 111-122.

Chimeh U., Zimmerman M.A., Gilyazova N. and Li P.A. (2018). B355252, a novel small molecule, confers neuroprotection against cobalt chloride toxicity in mouse hippocampal cells through altering mitochondrial dynamics and limiting autophagy induction. Int. J. Med. Sci. 15, 1384-1396.

Cui D., Wang L., Qi A., Zhou Q., Zhang X. and Jiang W. (2012). Propofol prevents autophagic cell death following oxygen and glucose deprivation in PC12 cells and cerebral ischemia-reperfusion injury in rats. PLoS One 7, e35324.

Cui D.R., Wang L., Jiang W., Qi A.H., Zhou Q.H. and Zhang X.L. (2013). Propofol prevents cerebral ischemia-triggered autophagy activation and cell death in the rat hippocampus through the NF-kappaB/p53 signaling pathway. Neuroscience 246, 117-132.

Engelhard K., Werner C., Eberspacher E., Pape M., Blobner M., Hutzler P. and Kochs E. (2004). Sevoflurane and propofol influence the expression of apoptosis-regulating proteins after cerebral ischaemia and reperfusion in rats. Eur. J. Anaesthesiol. 21, 530-537.

Gamdzyk M., Doycheva D.M., Araujo C., Ocak U., Luo Y., Tang J. and Zhang J.H. (2020). cGAS/STING pathway activation contributes to delayed neurodegeneration in neonatal hypoxia-ischemia rat model: Possible involvement of LINE-1. Mol. Neurobiol. 57, 2600-2619.

Gao X., Guo M., Meng D., Sun F., Guan L., Cui Y., Zhao Y., Wang X., Gu X., Sun J. and Qi S. (2019). Silencing microRNA-134 alleviates hippocampal damage and occurrence of spontaneous seizures after intraventricular kainic acid-induced status epilepticus in rats. Front. Cell Neurosci. 13, 145.

Goloshvili G., Barbakadze T. and Mikeladze D. (2019). Sodium nitroprusside induces H-ras depalmitoylation and alters the cellular response to hypoxia in differentiated and undifferentiated PC12 cells. Cell Biochem. Funct. 37, 545-552.

Gozal E., Metz C.J., Dematteis M., Sachleben L.R., Jr., Schurr A. and Rane M.J. (2017). PKA activity exacerbates hypoxia-induced ROS formation and hypoxic injury in PC12 cells. Toxicol. Lett. 279, 107-114.

Guidi G., Schiavon R., Sheiban I. and Perona G. (1986). Platelet glutathione peroxidase activity is impaired in patients with coronary heart disease. Scand. J. Clin. Lab. Invest. 46, 549-551.

Hajiahmadi S., Panjehpour M., Aghaei M. and Shabani M. (2015). Activation of A2b adenosine receptor regulates ovarian cancer cell growth: Involvement of Bax/Bcl-2 and caspase-3. Biochem. Cell Biol. 93, 321-329.

Hartwig K., Fackler V., Jaksch-Bogensperger H., Winter S., Furtner T., Couillard-Despres S., Meier D., Moessler H. and Aigner L. (2014). Cerebrolysin protects PC12 cells from $CoCl_2$-induced hypoxia employing GSK3beta signaling. Int. J. Dev. Neurosci. 38, 52-58.

Huang W., Liu X., Cao J., Meng F., Li M., Chen B. and Zhang J. (2015). Mir-134 regulates ischemia/reperfusion injury-induced neuronal cell death by regulating creb signaling. J. Mol. Neurosci. 55, 821-829.

Huang X., Teng Y., Yang H. and Ma J. (2016). Propofol inhibits invasion and growth of ovarian cancer cells via regulating mir-9/NF-kappaB signal. Braz. J. Med. Biol. Res. 49, e5717.

Ishikawa M., Tanaka S., Arai M., Genda Y. and Sakamoto A. (2012). Differences in microRNA changes of healthy rat liver between sevoflurane and propofol anesthesia. Anesthesiology 117, 1245-1252.

Jimenez-Mateos E.M., Engel T., Merino-Serrais P., Fernaud-Espinosa I., Rodriguez-Alvarez N., Reynolds J., Reschke C.R., Conroy R.M., McKiernan R.C., deFelipe J. and Henshall D.C. (2015). Antagomirs

targeting microRNA-134 increase hippocampal pyramidal neuron spine volume in vivo and protect against pilocarpine-induced status epilepticus. Brain Struct. Funct. 220, 2387-2399.

Kasai S., Richardson M.J.E., Torii S., Yasumoto K.I., Shima H., Igarashi K., Itoh K., Sogawa K. and Murayama K. (2017). Increase in proapoptotic activity of inhibitory PAS domain protein via phosphorylation by MK2. FEBS J. 284, 4115-4127.

Kim J.H., Kim B.K., Kim D.W., Shin H.Y., Yu S.B., Kim D.S., Ryu S.J., Kim K.H., Jang H.K. and Kim J.D. (2014). Effect of propofol on microRNA expression profile in adipocyte-derived adult stem cells. Chonnam Med. J. 50, 86-90.

Kungys G., Kim J., Jinks S.L., Atherley R.J. and Antognini J.F. (2009). Propofol produces immobility via action in the ventral horn of the spinal cord by a gabaergic mechanism. Anesth. Analg. 108, 1531-1537.

Lahiani A., Hidmi A., Katzhendler J., Yavin E. and Lazarovici P. (2016). Novel synthetic pegylated conjugate of alpha-lipoic acid and tempol reduces cell death in a neuronal pc12 clonal line subjected to ischemia. ACS Chem. Neurosci. 7, 1452-1462.

Lahiani A., Zahavi E., Netzer N., Ofir R., Pinzur L., Raveh S., Arien-Zakay H., Yavin E. and Lazarovici P. (2015). Human placental expanded (PLX) mesenchymal-like adherent stromal cells confer neuroprotection to nerve growth factor (NGF)-differentiated pc12 cells exposed to ischemia by secretion of IL-6 and VEGF. Biochim. Biophys Acta 1853, 422-430.

Medina V., Edmonds B., Young G.P., James R., Appleton S. and Zalewski P.D. (1997). Induction of caspase-3 protease activity and apoptosis by butyrate and trichostatin a (inhibitors of histone deacetylase): Dependence on protein synthesis and synergy with a mitochondrial/cytochrome c-dependent pathway. Cancer Res. 57, 3697-3707.

Meng F., Li Y., Chi W. and Li J. (2016). Morphine preconditioning downregulates microRNA-134 expression against oxygen-glucose deprivation injuries in cultured neurons of mice. J. Neurosurg. Anesthesiol. 28, 195-202.

Morris G., Brennan G.P., Reschke C.R., Henshall D.C. and Schorge S. (2018). Spared CA1 pyramidal neuron function and hippocampal performance following antisense knockdown of microRNA-134. Epilepsia 59, 1518-1526.

Nakashima A., Tanaka N., Tamai K., Kyuuma M., Ishikawa Y., Sato H., Yoshimori T., Saito S. and Sugamura K. (2006). Survival of parvovirus B19-infected cells by cellular autophagy. Virology 349, 254-263.

Richter C. (1993). Pro-oxidants and mitochondrial Ca^{2+}: Their relationship to apoptosis and oncogenesis. FEBS Lett. 325, 104-107.

Rodriguez A.S., Engel T., Palfi A., Farrar G.J., Henshall D.C. and Jimenez-Mateos E.M. (2017). Tubby-like protein 1 (Tulp1) is a target of microRNA-134 and is down-regulated in experimental epilepsy. Int. J. Physiol. Pathophysiol. Pharmacol. 9, 178-187.

Roy C.S. and Sherrington C.S. (1890). On the regulation of the blood-supply of the brain. J. Physiol. 11, 85-158 117.

Sada K., Nishikawa T., Kukidome D., Yoshinaga T., Kajihara N., Sonoda K., Senokuchi T., Motoshima H., Matsumura T. and Araki E. (2016). Hyperglycemia induces cellular hypoxia through production of mitochondrial ros followed by suppression of aquaporin-1. PLoS One 11, e0158619.

Schrouff J., Perlbarg V., Boly M., Marrelec G., Boveroux P., Vanhaudenhuyse A., Bruno M.A., Laureys S., Phillips C., Pelegrini-Issac M., Maquet P. and Benali H. (2011). Brain functional integration decreases during propofol-induced loss of consciousness. Neuroimage 57, 198-205.

Sun J., Gao X., Meng D., Xu Y., Wang X., Gu X., Guo M., Shao X., Yan H., Jiang C. and Zheng Y. (2017). Antagomirs targeting miroRNA-134 attenuates epilepsy in rats through regulation of oxidative stress, mitochondrial functions and autophagy. Front. Pharmacol. 8, 524.

Sun B., Ou H., Ren F., Huan Y., Zhong T., Gao M. and Cai H. (2018). Propofol inhibited autophagy through Ca(2+)/caMKKbeta/AMPK/mTOR pathway in ODG/R-induced neuron injury. Mol. Med. 24, 58.

Twaroski D.M., Yan Y., Olson J.M., Bosnjak Z.J. and Bai X. (2014). Down-regulation of microRNA-21 is involved in the propofol-induced neurotoxicity observed in human stem cell-derived neurons. Anesthesiology 121, 786-800.

Uchiyama Y. (2001). Autophagic cell death and its execution by lysosomal cathepsins. Arch. Histol. Cytol. 64, 233-246.

Wang Z., Yang P. and Qi Y. (2015). Role of microRNA-134 in the neuroprotective effects of propofol against oxygen-glucose deprivation and related mechanisms. Int. J. Clin. Exp. Med. 8, 20617-20623.

Wang P., Zhao R., Yan W., Zhang X., Zhang H., Xu B., Chu F., Han Y., Li G., Liu W., Zhang Y. and Lei H. (2018). Neuroprotection by new ligustrazine-cinnamon acid derivatives on $CoCl_2$-induced apoptosis in differentiated PC12 cells. Bioorg. Chem. 77, 360-369.

Wang C., Wan H., Wang Q., Sun H., Sun Y., Wang K. and Zhang C. (2020). Safflor yellow B attenuates ischemic brain injury via downregulation of long noncoding AK046177 and inhibition of microRNA-134 expression in rats. Oxid. Med. Cell. Longev. 2020, 4586839.

Wohaieb S.A. and Godin D.V. (1987). Starvation-related alterations in free radical tissue defense mechanisms in rats. Diabetes 36, 169-173.

Xiao L., Lan A., Mo L., Xu W., Jiang N., Hu F., Feng J. and Zhang C. (2012). Hydrogen sulfide protects PC12 cells against reactive oxygen species and extracellular signal-regulated kinase 1/2-mediated downregulation of glutamate transporter-1 expression induced by chemical hypoxia. Int. J. Mol. Med. 30, 1126-1132.

Yamanaka-Tatematsu M., Nakashima A., Fujita N., Shima T., Yoshimori T. and Saito S. (2013). Autophagy induced by HIF1α overexpression supports trophoblast invasion by supplying cellular energy. PloS One 8, e76605.

Yang T., Li D., Liu F., Qi L., Yan G. and Wang M. (2015). Regulation on beclin-1 expression by mtor in $CoCl_2$-induced HT22 cell ischemia-reperfusion injury. Brain Res. 1614, 60-66.

Zalewska T., Jaworska J., Sypecka J. and Ziemka-Nalecz M. (2020). Impact of a histone deacetylase inhibitor—trichostatin a on neurogenesis after hypoxia-ischemia in immature rats. Int. J. Mol. Sci. 21, 3808.

Accepted January 7, 2021